Supporting Information

Synthesis of recoverable thermosensitive Fe_3O_4 hybrid microgels with controllable catalytic activities

Jing Chen, *[a] Xiaozhen Ma, [a,b] Pitchaimari Gnanasekar, [c] Dongdong Qin, [a,d] Qing Luo, [a] Zhong Sun, [e] Jin Zhu [a] and Ning Yan *[c]

[a] Key Laboratory of Bio-based Polymeric Materials Technology and Application of Zhejiang Province, Division of Polymer and Composite Materials, Ningbo Institute of Material Technology and Engineering, Chinese Academy of Science, Zhejiang, Ningbo 315201, P. R. China

[b] University of Chinese Academy of Sciences, Beijing 100049, P. R. China

[c] Department of Chemical Engineering and Applied Chemistry, University of Toronto, 200 College street, ON M5S 3E5, Canada

[d] School of Chemical Engineering & Technology, Tianjin University, Tianjin 300350, P. R. China

[e] College of Chemical Engineering, Sci-Tech Center for Clean Conversion and High-Value Utilization of Biomass, Northeast Electric Power University, Jilin 132012, P. R. China

Contact: chenjing@nimte.ac.cn and ning.yan@utoronto.ca

Experimental section

1.1 Materials

All chemicals were available of analytical grade or highest purity. 3-(trimethoxysilyl)propyl methacrylate (KH-570) was obtained from Tokyo Chemical Industry (TCI) (Japan). Chloroauric acid ($HAuCl_4$), sodium borohydride ($NaBH_4$) and 4-nitrophenol were purchased from Sinopharm Chemical Reagent Co., Ltd. (Shanghai, China) and used as received. 2-dimethylaminoethyl methacrylate (DMAEMA) was purchased from the Energy Chemical Company (Shanghai, China). All materials were used as received without further purification.

1.2 Preparation of double bond modified Fe_3O_4 nanoparticles (NPs)

Fe_3O_4 NPs were synthesized according to the previous report. [1] In a round bottom flask, Fe_3O_4 (0.5 g) and KH-570 (0.3 mL) were dissolved in ethanol (45 mL) and stirred for 24 h at room temperature. Afterward, the solution was washed with ethanol by centrifugation (1600 rpm) six times to remove the unreacted reactants, etc. Finally, Fe_3O_4 NPs were dried in an oven at 60 ºC.

1.3 SIPGP

The modified Fe_3O_4@PDMAEMA microgel was synthesized through SIPGP just like the previous work. [2] Polymerizations were carried out in a round-bottom tube (50 mL) equipped with a magnetic stirrer. A mixture of monomer (DMAEMA) (2 mL) and KH-570 modified Fe_3O_4 NPs (20 mg) was added into the test tube under constant stirring (250 rpm). The tube was placed under an ultraviolet lamp and irradiated at room temperature for 40 minutes. A high-pressure mercury lamp purchased from

Jiguang Co. (Shanghai, China) was applied for SIPGP. Its wavelength ranged from 200 to 400 nm. The distance between the light source and the reaction mixture was 10 cm. After the completion of the polymerization, the microgels were purified via five cycles of centrifugation/redispersion in acetone at 8000 rpm. The Fe_3O_4@PDMAEMA microgel was collected and dried in vacuum at 80°C for 24 h before characterization.

1.4 Fe_3O_4@PDMAEMA for the loading of gold NPs

The synthesis of Au NPs within the prepared microgels was described in detail as follows: 50mg of Fe_3O_4@PDMAEMA were first dispersed in 10 mL of deionized water. Afterward, 0.25 mL of 4 mM $HAuCl_4$ aqueous solution was added. And the mixture was stirred for 1 h after adding 1 mL of 0.05 M $NaBH_4$ aqueous solution dropwise under the ice water bath. Any excess of $HAuCl_4$ was removed by centrifugation, decantation, and washing with water to prevent the formation of extraneous Au nanoparticles on the outside of the microgels. The final microgel was dried under vacuum until reaching a constant weight.

1.5 Catalytic Reduction of 4-Nitrophenol to 4-Aminophenol in an Aqueous Medium

As a model reaction, we chose the reduction of 4-nitrophenol (4-NP) to 4-aminophenol (4-AP) using $NaBH_4$**.** A typical experiment was carried out as follows: 1.0 mL of $NaBH_4$ (0.2M, 2×10^{-4} mol) aqueous solution, 0.1 mL of 4-NP aqueous solution (5 mM, 5×10^{-7} mol) and 2.0 mL of water were mixed in a glass vial. Then, 0.05 mL of catalyst dispersion (1.0 mg/mL) was added directly into the solution to

start the reaction. With the progress of the catalytic reaction, the bright-yellow solution faded gradually. The activity of the catalyst was monitored by a UV-vis spectrophotometer with the extinction at 400 nm in UV-vis absorbance and an increase in the absorption at 300 nm at the same time, demonstrating the formation of 4-AP.

1.6 Characterizations

The morphology and size of the samples were investigated using transmission electron microscopy (TEM, Tecnai F20 S-TWIN (FEI), USA, accelerating voltage of 200 kV). TEM samples were prepared by dropping a diluted aqueous solution (5μL) of samples onto carbon-coated copper grids and were dried in air for 1h. The energy-dispersive X-ray (EDX) elemental mapping images of individual Fe_3O_4@PDMAEMA/Au were obtained using JEOL JEM-2200FS (Peabody, MA). Fourier transform infrared spectroscopy (FT-IR, Nicolet 6700, Thermoscientific, USA) was used to collect absorbance spectra over a frequency range of 4000-500 cm^{-1} at room temperature. For each sample, 1000 scans were taken at a spectral resolution of 4 cm^{-1} with an induction time of 20 min for N_2 exposure (to eliminate noise from atmospheric water). The background spectra were recorded on the corresponding KBr disks. Scanning electronic microscopy measurements were carried out using a scanning microscope (SEM, JMS-7600F, JEOL, Japan). Thermogravimetric analysis was carried out on a TGA/DSC I instrument (TGA, Mettler Toledo, Switzerland) with a heating rate of 10 ^oC min^{-1} in flowing N_2 and a sample of 3-5 mg. Dynamic light scattering analysis was performed using a Zetasizer Nano instrument (DLS, Malvern,

UK) with a laser light wavelength of 633 nm, and all data were measured over four measurements. UV-vis absorption spectra of the samples were recorded using a spectrophotometer (Lambda 950, Perkin-Elmer, USA). Measurements of the solutions were taken in 3mL quartz cuvettes. Besides, magnetic measurements at 300 K were carried out using a vibrating sample magnetometer (VSM, 7400 Series, Lakeshore, USA). X-ray Photoelectron spectrum (XPS, AXIS ULTRA DLD, Kratos Analytical Ltd., Manchester, UK) measurements were carried out under pressure between 10^{-9} and 10^{-8} mbar. The system was equipped with a monochromatic Al Ka source and all peaks are referenced to the signature of the C 1s peak for carbon at 284.8 eV. Fe and Au content of Fe_3O_4@PDMAEMA/Au were determined by Inductively Coupled Plasma-Atomic Emission Spectrometry (ICP-AES) using a Germany SPECTRO ARCOS II instrument.

Figures

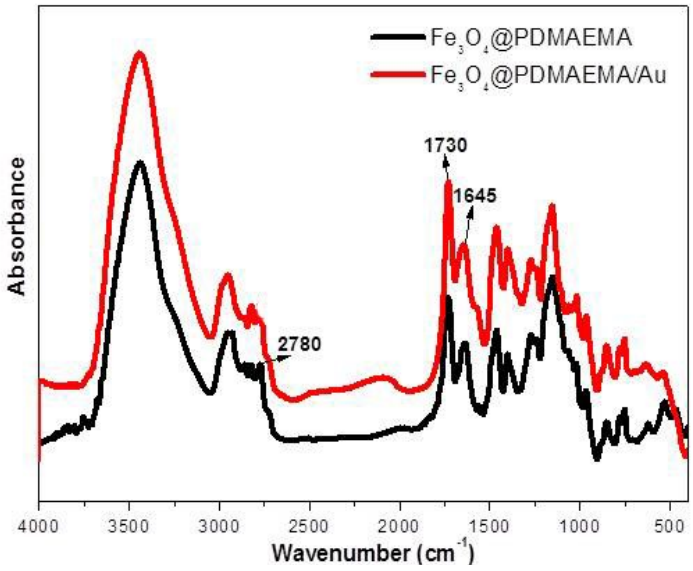

Fig.S1 FT-IR spectra of (black) Fe_3O_4@PDMAEMA and (red) Fe_3O_4@PDMAEMA/Au.

According to the results in Figure S1, there is no significant difference between FTIR spectra of Fe_3O_4@PDMAEMA and Fe_3O_4@PDMAEMA/Au except the peak at 2780 cm^{-1} related to the C-H stretching vibrations of the N-CH_3 groups of PDMAEMA brushes disappeared. It may be due to the interaction between Fe_3O_4@PDMAEMA and Au nanoparticles. Also, this disappeared absorption means that the N-CH_3 group is reduced to quaternary amines or other coordination compounds. Therefore, the end tertiary amine groups of PDMAEMA are considered to be the main reason for the reduction reaction between PDMAEMA and $HAuCl_4$. Meanwhile, this result is similar to our previous work. [3]

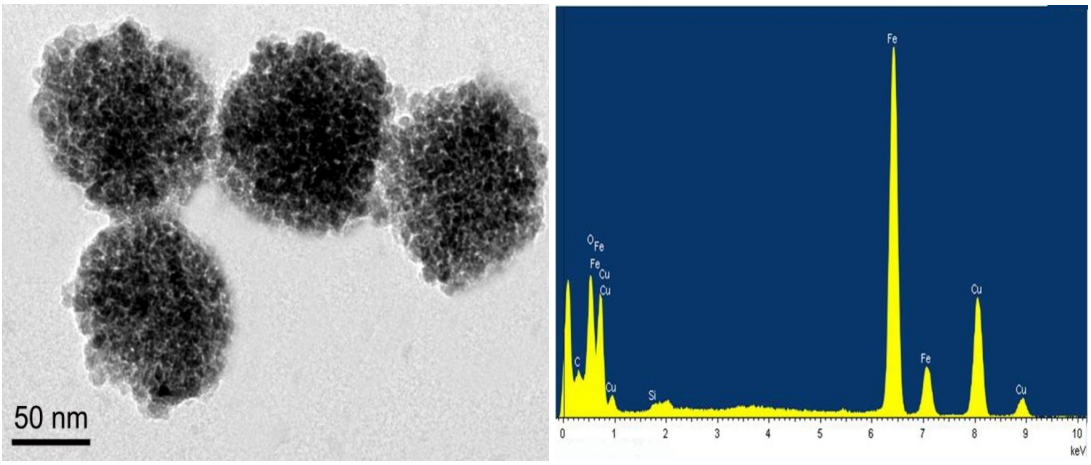

Fig.S2 TEM image and EDX spectrum of Fe_3O_4. The copper peaks are from the copper grid used as support in the measurements.

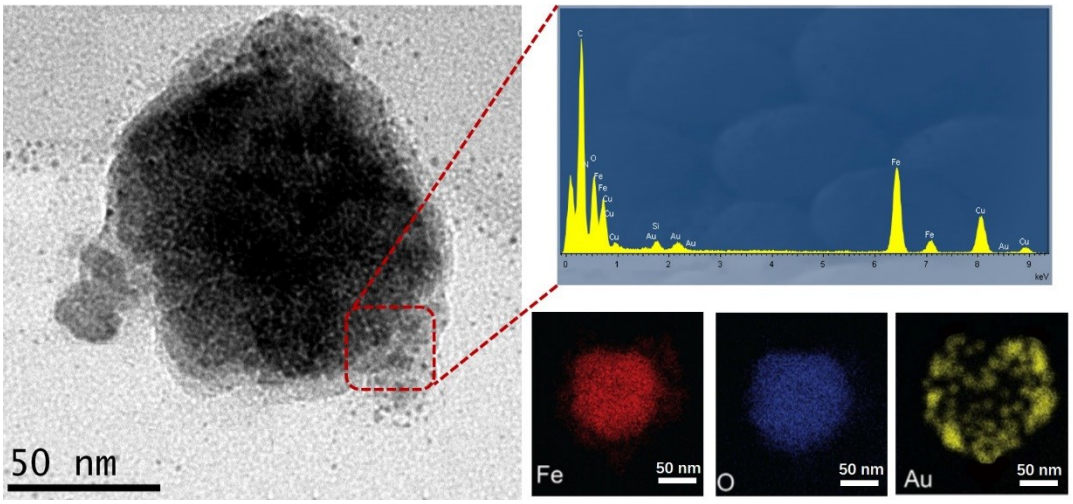

Fig.S3 TEM image (a) and EDX spectrum (b) of Fe_3O_4@PDMAEMA/Au. The copper peaks are from the copper grid used as support in the measurements. (c) EDX elemental mapping images of Fe_3O_4@PDMAEMA/Au based on Fe, O, and Au element at the same area.

As shown in the energy-disperse X-ray (EDX) pattern of the Fe_3O_4@PDMAEMA/Au hybrid together with the elemental mapping data of gold (Figure S3), the distributed signals from Au further confirmed the well dispersion of gold nanoparticles in the hybrid system.

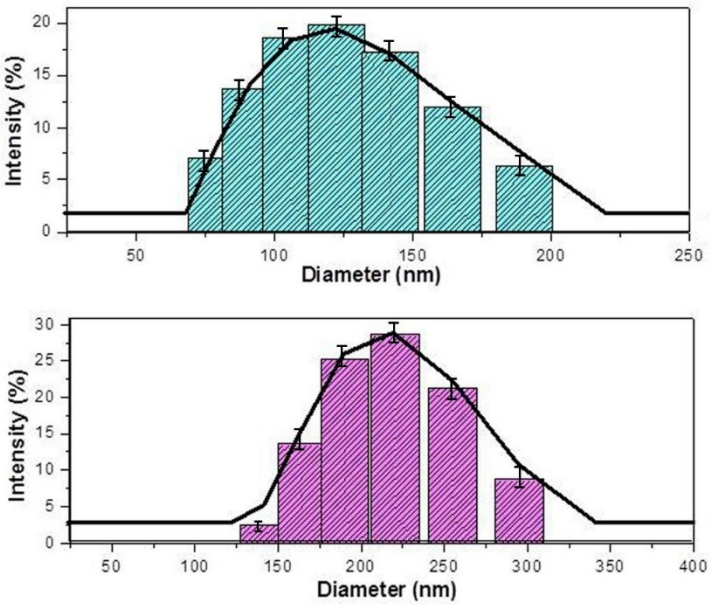

Fig.S4 Particle size for Fe_3O_4 (green) and Fe_3O_4@PDMAEMA (purple).

The average sizes are 123.5±60.5 nm and 254.8±50.2 nm, and polydispersity index are 1.8 and 1.5, respectively, which are consistent with the SEM and TEM results.

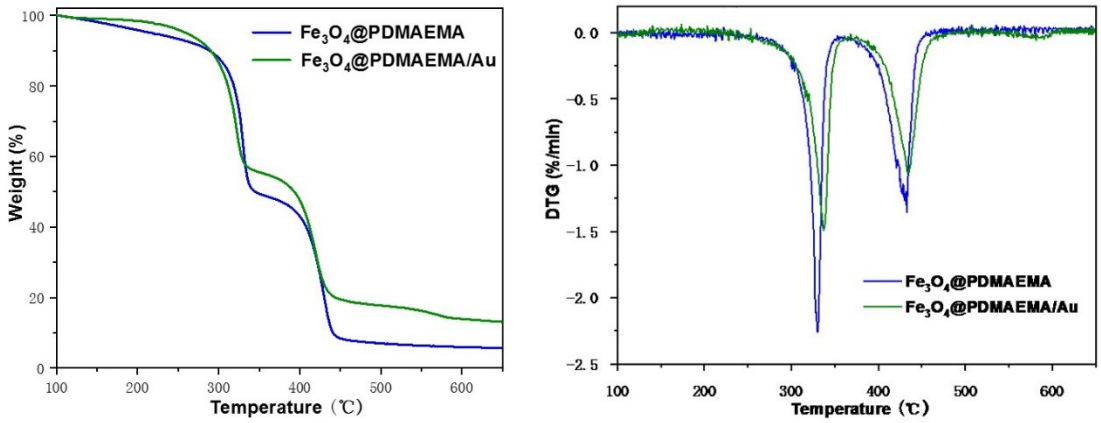

Fig.S5 TGA and DTG of Fe_3O_4@PDMAEMA (blue) and Fe_3O_4@PDMAEMA/Au (green).

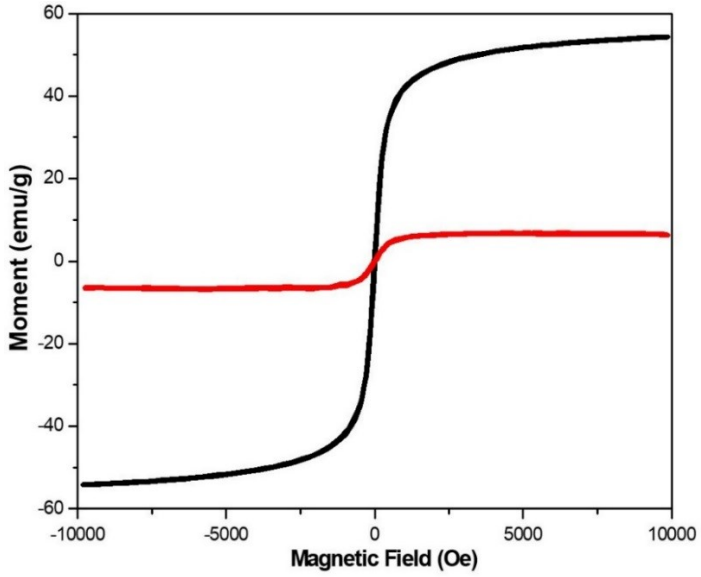

Fig.S6 Magnetization curves of Fe_3O_4 nanoparticles (black line) and Fe_3O_4@PDMAEMA (red line) at 2 °C (300 K).

As shown in Figure S6, the magnetic hysteresis loops of Fe_3O_4 and Fe_3O_4@PDMAEMA reveal that they possess superparamagnetic behavior, and their saturation magnetization moments reach 54.29 and 3.5 emu/g, respectively. The magnetization plateau for Fe_3O_4@PDMAEMA nanocomposites is considerably lower due to the higher shielding effect of the PDMAEMA shell and the low magnetite content of Fe_3O_4 (TGA data Figure 3) in the polymeric microgels. But the magnetization curves also indicate that the iron oxide inside the microgels has sufficient magnetic properties. This experimental data is consistent with findings from previous literature reports. [4-5] Meanwhile, this result indicates that Fe_3O_4@PDMAEMA can be efficiently separated by an external permanent magnet.

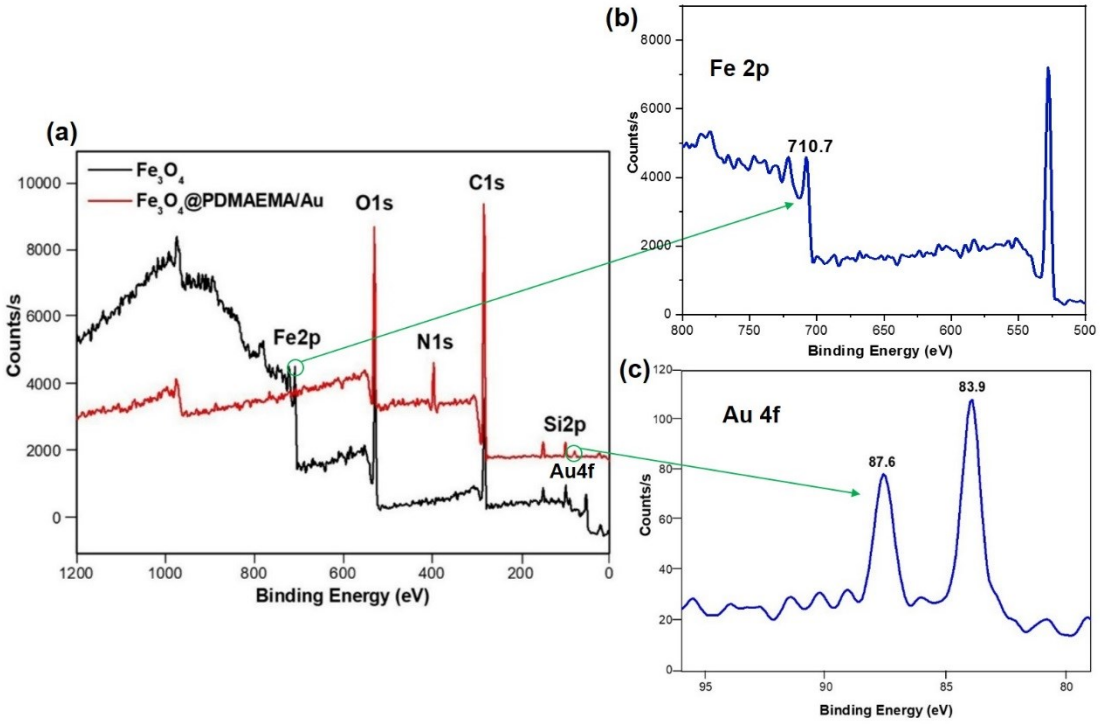

Fig.S7 XPS spectra of (a) Fe_3O_4 (black) and Fe_3O_4@PDMAEMA/Au (red). (b) Fe 2p XPS spectra of Fe_3O_4. (c) Au 4f XPS spectra of Fe_3O_4@PDMAEMA/Au system.

The signals at the Fe 2p regions and the peak of Fe $2p_{3/2}$ at 710.7 eV indicate that both Fe^{2+} and Fe^{3+} exist showing the formation of Fe_3O_4 in Figure S7a-b. For Fe_3O_4@PDMAEMA, there is a peak at 399.8 eV, corresponding to the N1s binding energy of PDMAEMA chains. However, the XPS spectrum of Fe_3O_4 shows no peak at 399.8 eV, which implies that the surfaces of Fe_3O_4@PDMAEMA have been successfully functionalized with PDMAEMA. Meanwhile, the absence of Fe 2p at 710.7 eV further supported that all the Fe_3O_4 cores were fully confined within the PDMAEMA shell. The corresponding C1s binding energy of Fe_3O_4 and Fe_3O_4@PDMAEMA nanocomposite is also shown in Figure S7a. In Figure S7c, the Au $4f_{7/2}$ and Au $4f_{5/2}$ peaks appeared at 83.9 eV and 87.6 eV, respectively, are following the characteristic peaks for the metallic Au^0 state.

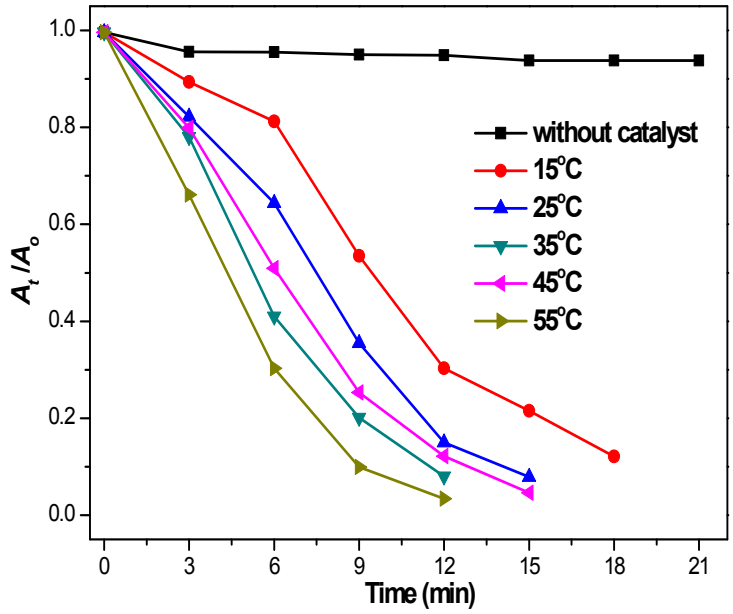

Fig.S8 A_t /A_0 versus reaction time for the reduction of 4-NP over no catalyst and Fe_3O_4@PDMAEMA/Au at different temperatures. A_0 and A_t are the absorption peak at 400 nm initially and at time t.

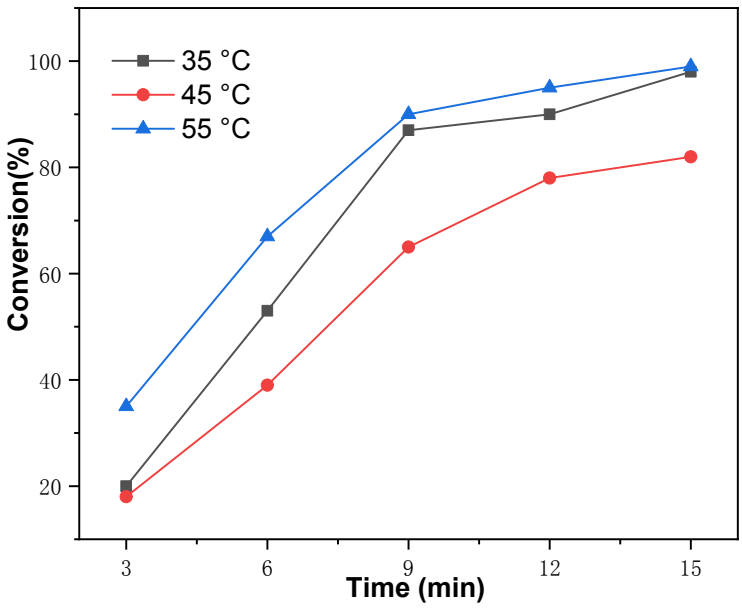

Fig.S9 The conversion of 4-NP at different temperatures catalyzed by Fe_3O_4@PDMAEMA/Au. The composite particles consisting of thermo-sensitive core-shell structures in which Au NPs are embedded. When T > 40 °C, the network shrinks

and the catalytic activity of the nanoparticles is strongly affected in this cyclic manner.

As observed from Figure S9, when T <LCST, the catalyst was found to be more effective for catalytic reduction (35 °C, 6 min, conversion = 53%), whereas when T > LCST, the reduction rate significantly decreased (45 °C, 6 min, conversion = 39%). This suggested that the hydrophobic shell of PDMAEMA in the Fe_3O_4@PDMAEMA/Au system at a temperature above the LCST just decelerate but not stop the reactants reaching the surface of the gold catalyst. When temperature was further increased, the conversion at 55 °C is at about 67% in 6 min, possibly due to the complete collapse of PDMAEMA chains, limits the diffuse of reactants through the hydrophobic shell. In contrast, under their LCST, the grafted PDMAEMA chains will become hydrophilic, and are completely dissolved in the system, which lead to the 'exposure' of encapsulated Au NPs from PDMAEMA chains. These exposed Au NPs will enhance the catalytic capability.

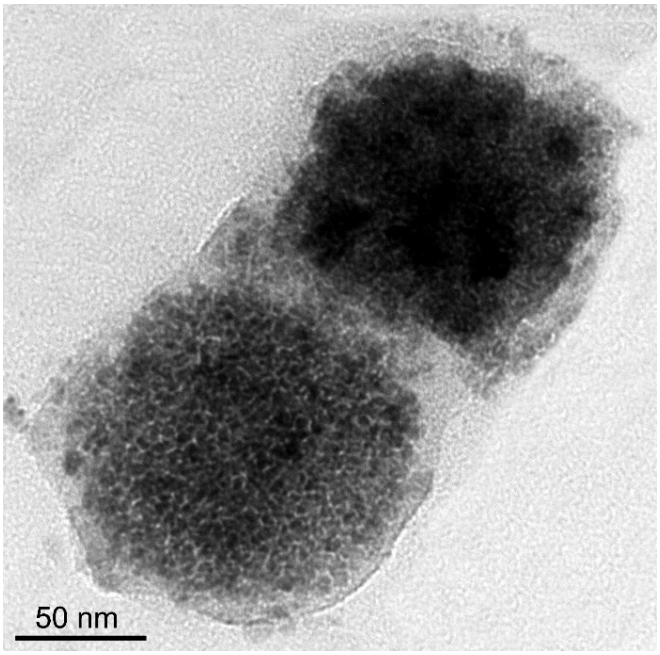

Fig.S10 TEM image of Fe_3O_4@PDMAEMA/Au after the catalytic test.

As shown in Figure S10, the Au NPs with the same size distribution (2-3 nm) compared with the catalyst before the reaction is uniformly supported on Fe_3O_4@PDMAEMA, indicating that the binding between Fe_3O_4@PDMAEMA and Au NPs is strong enough.

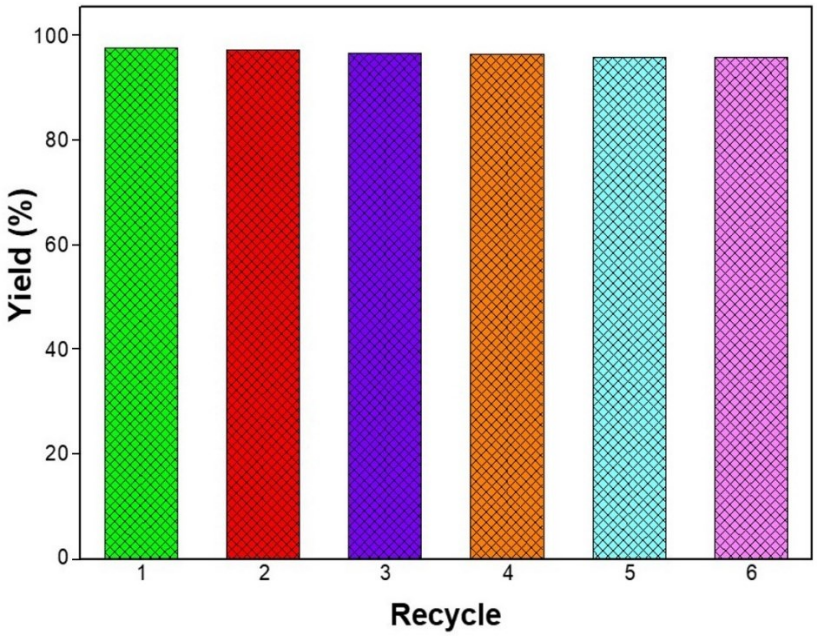

Fig.S11 The reusability of the catalyst was tested in six consecutive cycles and the catalytic condition was the same as our first catalytic condition (1.0 mL of $NaBH_4$ (0.2M, 2×10^{-4} mol) aqueous solution, 0.1 mL of 4-NP aqueous solution (5 mM, 5×10^{-7} mol) and 2.0 mL of water were mixed in a glass vial. Then, 0.05 mL of catalyst dispersion (1.0 mg/mL) was added directly into the solution to start the reaction). The catalyst was easily isolated from the reaction medium and cleaned with distilled water before being used in a new cycle. No differences in k_{app} were observed in any of the six cycles indicating that the activity remains unalterable for at least six cycles.

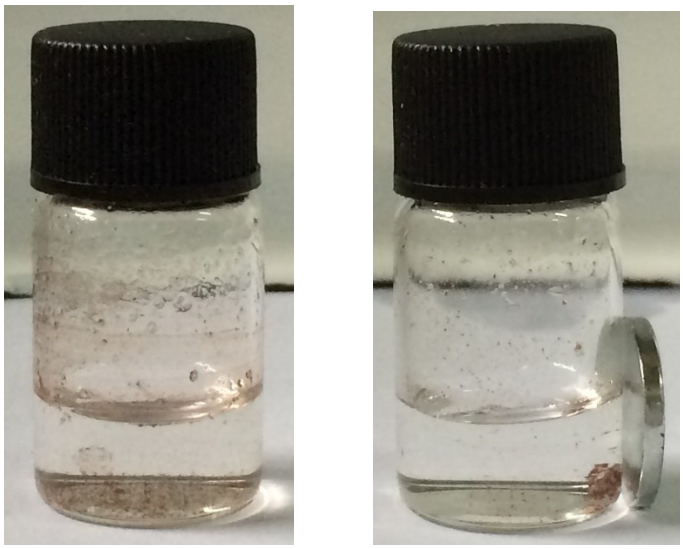

Fig.S12 Photographs showing the water dispersion of the catalyst (left) and concentration of nanocomposites on the right side of the vial by a magnet (right).

References

1 J. F. Zhang, A. H. Sun, X. X. Qiao, C. Y. Chu, C. Y. Wang, T. Chen, J. J. Guo, G. J. Xu, *Mater. Res. Express*, 2014, **1***,* 045037.

2 J. Chen, P. Xiao, J. C. Gu, D. Han, J. W. Zhang, A. H. Sun, W. Q. Wang, T. Chen, *Chem. Commun.*, 2014, **50**, 1212-1214.

3 J. Chen, P. Xiao, J. C. Gu, Y. J. Huang, J. W. Zhang, W. Q. Wang, T. Chen, *RSC Adv.,* 2014, **4**, 44480-44485.

4 C. A. Ribeiro, M. V. S. Martins, A. H. Bressiani, J. C. Bressiani, M. E. Leyva, A. A. A. de Queiroz, *Mat. Sci. Eng. C*, 2017, **81,** 156-166.

5 A. Pich, S. Bhattacharya, Y. Lu, V. Boyko, H. J. P. Adler, *Langmuir*, 2004, **20,** 10706-10711.